Supporting Information

Freezing-Induced Ice–Polymer Structuring Enables Tough, Additive-Free Hydrogels Under Extreme Cold Conditions

Jialun Wei[1], Dong Zhang[2], Yung Chang[3], Athena B Santi[1], Amanda Gomez[1], Lijin Wang[1], Gabriela Romero Uribe[1], Jie Zheng[1]*

[1]Department of Biomedical Engineering and Chemical Engineering, The University of Texas at San Antonio, Texas 78249, USA

[2]The Wallace H. Coulter Department of Biomedical Engineering, Georgia Institute of Technology, Georgia 30332, USA

[3]R&D Center for Membrane Technology and Department of Chemical Engineering, Chung Yuan Christian University, Chung-Li 32023, Taiwan

* E-mail: jie.zheng@utsa.edu

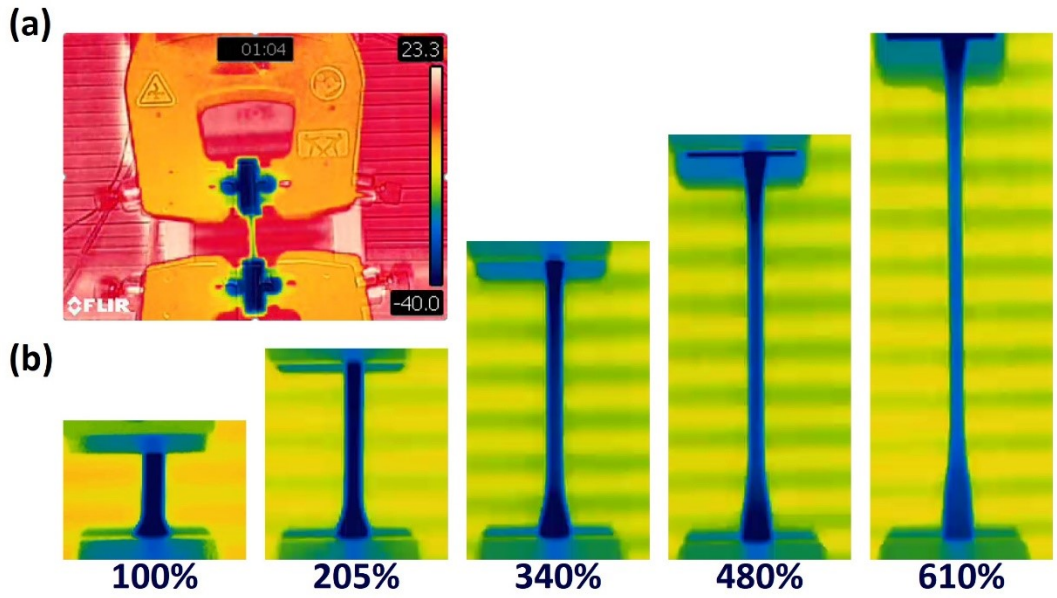

Fig. S1. Infrared thermal imaging of frozen gelatin/pNAGA hydrogels during tensile testing at room temperature. (a) Thermal image showing the setup immediately after mounting the frozen sample (t=0 s). Pre-cooled grips (-40 °C) were used to maintain the specimen temperature. **(b)** Temperature evolution during tensile testing up to 610% strain (total test duration t= ~60s). The gauge region remains within the dark blue range (-40 to -5 °C), demonstrating that the hydrogel remained fully frozen throughout the deformation and failure process.

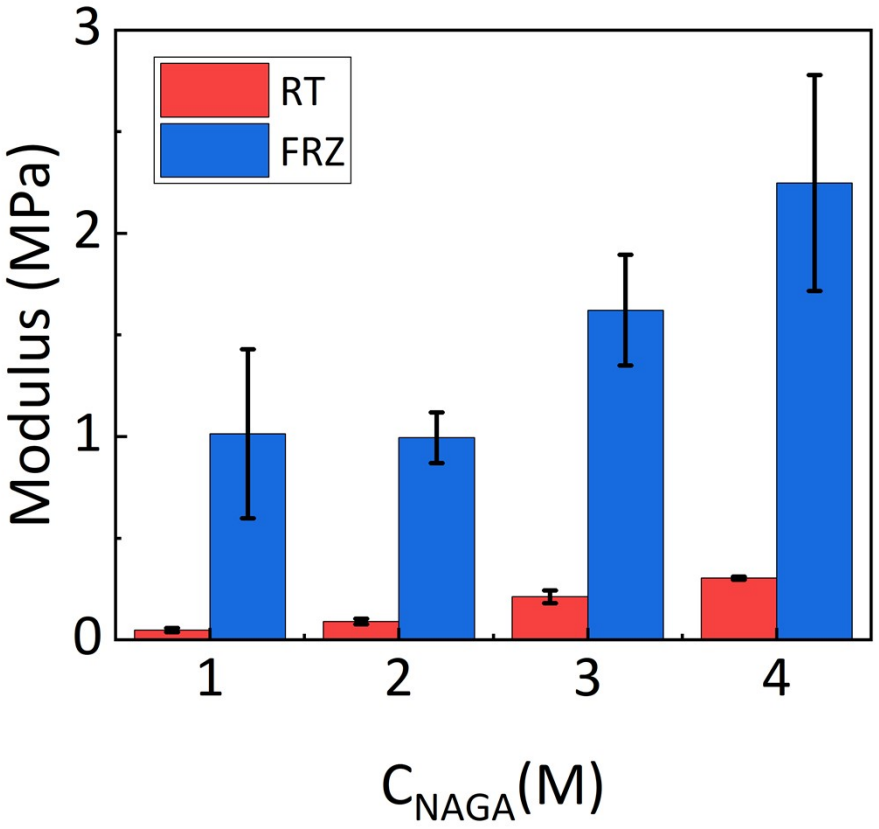

Fig. S2. Young's modulus of as-prepared and frozen DN hydrogels prepared with different concentration of NAGA (C_{NAGA}) and a fixed concentration of gelatin ($C_{gelatin}$=80 mg/mL). Error bars represent the standard deviation (n=3).

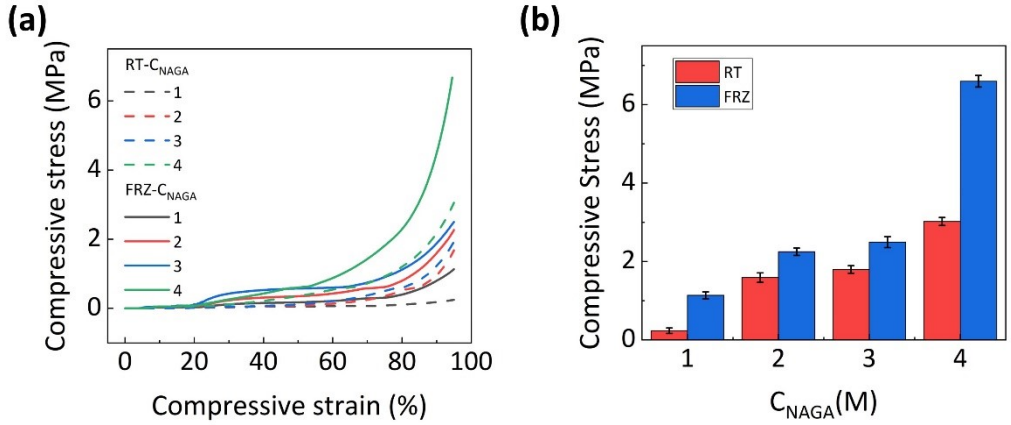

Fig. S3. (a) Compression strain-stress of as-prepared DN hydrogels and frozen hydrogels prepared with different C_{NAGA} and a fixed $C_{gelatin}$=80 mg/mL. **(b)** Corresponding maximum stress at 95% compression. Error bars represent the standard deviation (n=3).

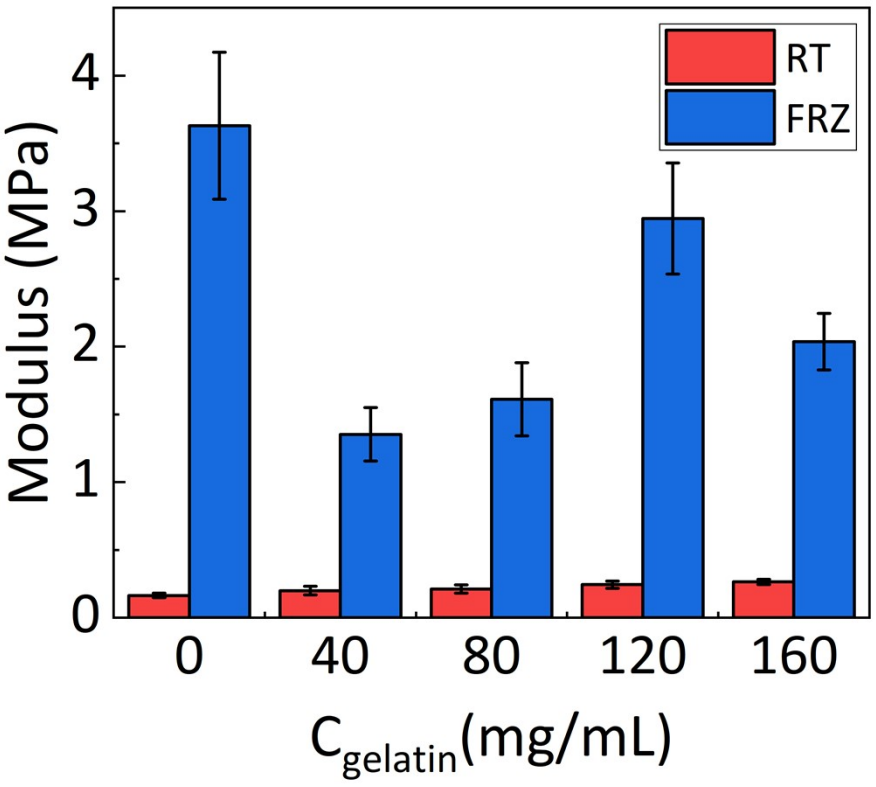

Fig. S4. Young's modulus of as-prepared and frozen DN hydrogels prepared with different concentration of gelatin ($C_{gelatin}$) and a fixed concentration of NAGA (C_{NAGA}=3 M). Error bars represent the standard deviation (n=3).

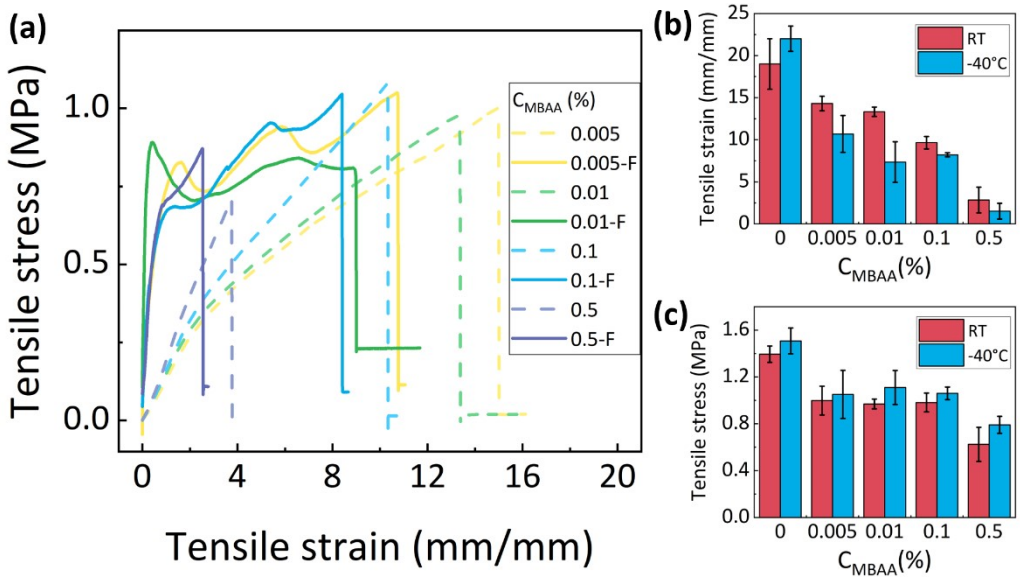

Fig. S5: Effect of chemical crosslinker concentration (CMBAA) on tensile performance at room temperature (RT) and -40 °C. (a) Representative tensile stress–strain curves of hydrogels with varying CMBAA (0–0.5%). Dashed lines denote RT, and solid lines denote -40 °C. **(b)** Corresponding maximum tensile strain and **(c)** tensile stress as a function of CMBAA under RT and -40 °C.

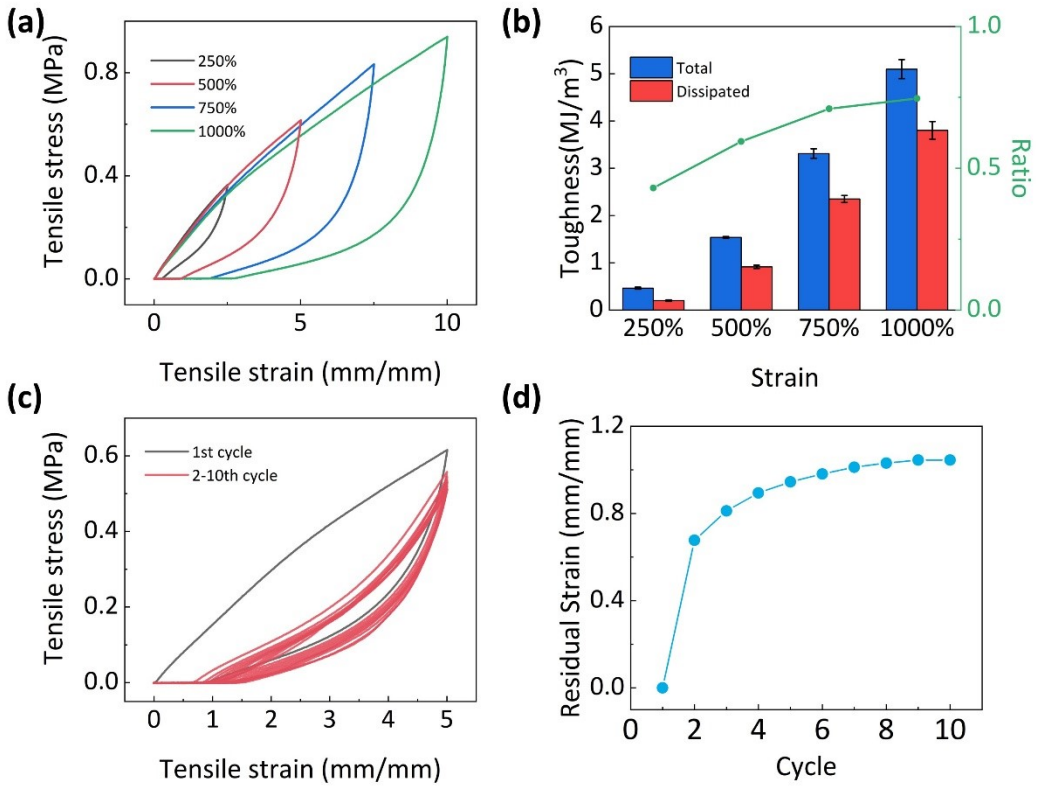

Fig. S6. Room temperature **(a)** Loading-unloading curves at different strain and **(b)** corresponding dissipated energy of DN hydrogels prepared at fixed composition of C_{NAGA}=3 M and $C_{gelatin}$=80 mg/mL. **(c)** Successive loading-unloading curves at 500% strain and (d) corresponding residual strain.

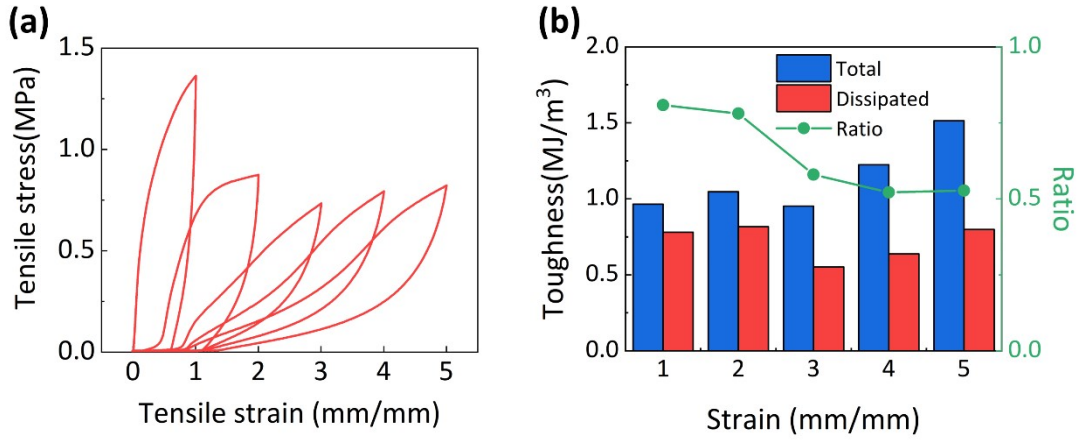

Fig. S7. Successive loading–unloading cycles of frozen gelatin/pNAGA DN hydrogels prepared at -40°C with composition of C_{NAGA}=3 M and $C_{gelatin}$=80 mg/mL under increasing strain. (a) Successive loading–unloading curves with maximum strain increasing from 1 to 5 mm/mm. **(b)** Corresponding total toughness (blue bar) and dissipated energy (red bar) as a function of strain. The green dots and right axis show the dissipation ratio. The results show a high dissipation ratio (~80%) at low strains (1–2 mm/mm) due to the fracture of the rigid ice crystals, which decreases and stabilizes (~50%–58%) at higher strains as the elasticity of the polymer network becomes dominant.

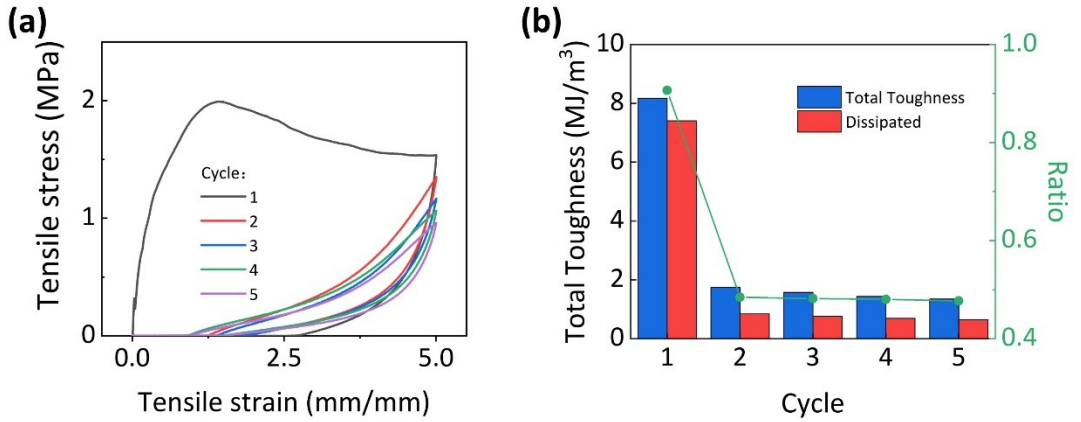

Fig. S8. Consecutive loading–unloading cycles of frozen gelatin/pNAGA DN hydrogels prepared at -40°C with composition of C_{NAGA}=3 M and $C_{gelatin}$=80 mg/mL at a fixed strain of 5 mm/mm. (a) Consecutive loading–unloading curves (cycles 1–5). **(b)** Evolution of total toughness (area under loading curve, blue bar) and dissipated toughness (hysteresis area, red bar) with cycle number. The green dot and right axis show the dissipation ratio of dissipated energy/total input energy. The data reveal pronounced Mullins-like softening: the first cycle exhibits markedly higher stiffness and a very large hysteresis loop due to sacrificial ice-crystal fracture, while subsequent cycles almost perfectly overlap with greatly reduced and stable toughness and dissipation.

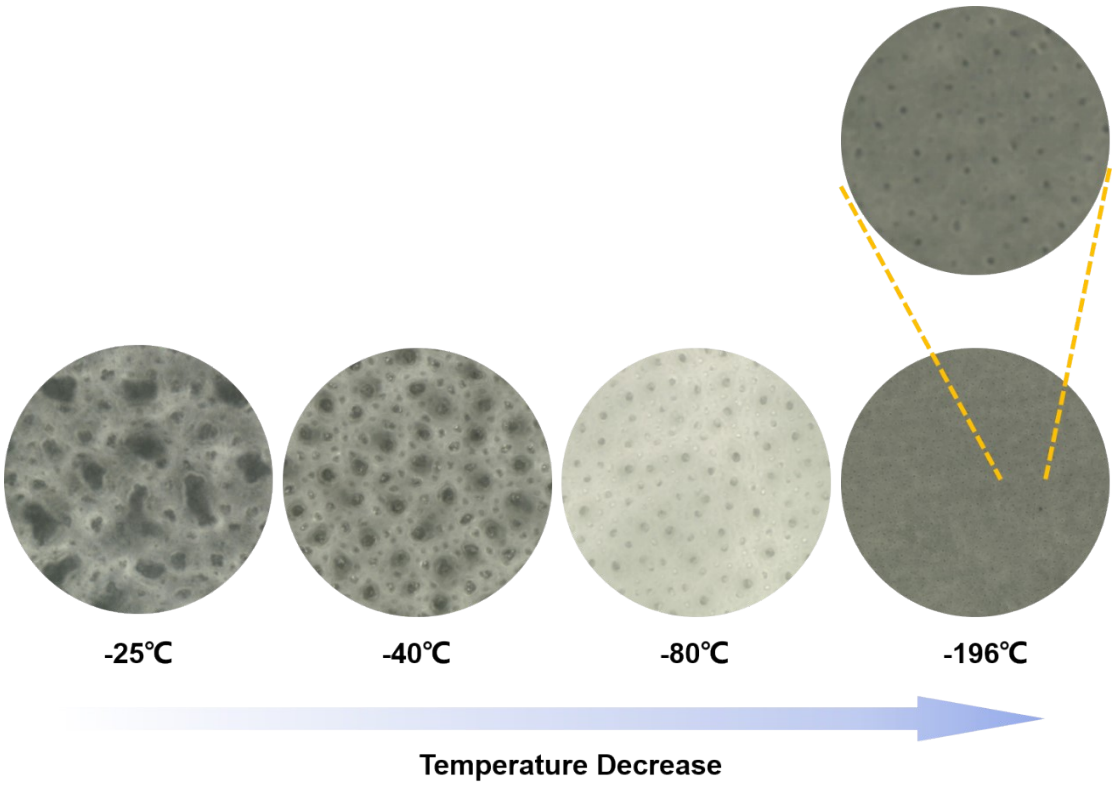

Fig. S9. Microscopic morphology of hydrogels frozen at different temperatures and observed after thawing, showing pore structures previously occupied by ice crystals.

Table S1: Summary of representative antifreezing hydrogel systems reported in the literature, including hydrogel composition, category (additive-free, organogel, protein-assisted, ionic, or nanocomposite), operating temperature, and tensile mechanical properties (strain and stress). Data correspond to the entries plotted in **Fig. 9**.

Gel Type	Polymer Network	Additives	T (°C)	Stress (MPa)	Strain (%)	Ref.
Intrinsic Polymer Hydrogels	Gelatin/pNAGA	–	-40	1.5~2.3	1000~2200	This Work
	EGINA-Crosslinked DN Hydrogels	–	-20	0.1~0.65	200~3000	48
	PDMAAPS	–	-20	0.1	2000	62
	P(MMA-co-HEA)	–	-45~-20	2.2~25.3	69~850	63
	PSBMA	–	-20	0.19	1167	64
	P(AAm-co-MAAc)	–	-45	30	35	65
	poly(AM-co-SBMA)/PDADMAC	–	-10	0.2	800	66
	PVA/ poly(AM-co-ACHPES)	–	-20	0.5	550	67
Organogels	PVA/PAAc	Glycerol	-40	50	200	68
	PVA	DMSO	-30	20~30	40~400	69
	Gelatin/ PMAA	Glycerol	-23	0.4	300	70
	Gelatin/PU nanomesh	Glycerol	-80	1	250	71
	PAMPS/PAAm	Glycerol, Choline chloride	-20	0.41	335	72
	PAAm	Glycerol, betaine	-20	0.18	1934	73
	PVDF/P(AAm-co-AN-NaSS)	Glycerol	-20	2	700	74
	Cellulose	Glycerol	-40	2.11	846	75
Protein-assisted Hydrogels	P(AAm-co-AAc)	IBP, INP	-30~0	5.2~21.7	137.5~254.9	76
	P(AAm-co-AMPS)	AFPs	-10	0.05	1400	77
	P(AAm-co-MAANa)/PVA	AFPs	-15	0.06	1000	78
Ionic Hydrogels	PVA	Sodium lignosulfonate	-60	10	375	79
	Alg/PAAm	H_2SO_4	-100	0.65	300	80
	CMCS/PAAM	$ZnClO_4$	-30	0.15	320	81
	PHEA	KAc	-60~0	0.2~0.3	400~600	82
	PVA/PEI	LiCl	-80	0.01~0.02	7000~8000	83

	PAAc	Betaine, $AlCl_3$	-50	1.088	2026	84
	PVA	KCl	-10	1.36	172	85
	Silk fibroin	EMImAc	-50~-10	0.58~0.84	80~95	85
	Gelatin	$Ca(NO)_2$, $(NH_4)_2SO_4$	-80	2.17	297	86
	P(SBMA-co-HEA)	LiCl	-40	0.005	325	87
	P(HEA-co-AA)	LiCl, Sodium lignosulfonate	-18	0.685	2403	88
	P(SBMA-co-AA)	$ZnCl_2$	-60~-20	0.38~0.42	420~450	89
	P(AAm-co-SV)	SG,GA,SS	-35	0.055	1041	90
Nanocomposite Hydrogels	PAAc	CNC@HA, Proline	-30	1	750	91
	PVA/P(AAm-co-AMPS)	CNFs	-10	0.09	470	92
	PAAm	Nanocellulose	-40~-20	0.12	800	93
	PAAm	cellulose nanofibril	-50~-15	0.3~0.4	450~500	94
	P(AAm-co-AAc)	PDA-decorated carbon nanotubes	-20	0.055	520	95